Supporting information

Two Azido-Bridged [2 × 2] Cobalt(II) Grids Featuring Single-Molecule Magnet Behaviour

Zhilin Guo,[ab] Yi-Fei Deng,*[a] Yipei Zhang,[a] Zoe Pikramenou,[b] Yuan-Zhu Zhang*[a]

[a] Department of Chemistry, Southern University of Science and Technology (SUSTech), Shenzhen 518055, China.

[b] School of Chemistry, University of Birmingham, Edgbaston, Birmingham B15 2TT, United Kingdom.

Experimental Section

Materials and Physical Measurements.

3, 6-di(pyridin-2-yl)pyridazine (pydz) ligand and other chemicals are commercially available and used as received. 3,6-bis(3,5-dimethyl-1H-pyrazol-1-yl)pyridazine (pzdz) was synthesised according to the literature.[1] Elemental analyses (C, H, N) were measured by a vario EL cube CHNOS Elemental Analyzer Elementar Analysensysteme GmbH. FT-IR spectra were recorded in the range 600-4000 cm^{-1} on a Bruker tensor II spectrophotometer. Powder X-ray diffraction (PXRD) measurements were recorded on a Rigaku Smartlab X-ray diffractometer. A PXRD pattern for **1** could not be obtained due to the loss of CHCl$_3$ interstitial solvent molecules. Magnetic measurements were carried out with a SQUID MPMS3 magnetometer. Magnetic data were corrected for the diamagnetism of the sample holder and for the diamagnetism of the sample using Pascal's constants.[2]

Caution: Although no such behavior was observed during the experiment, azido salts are potentially explosive and should be handled with care.

Synthesis of {[Co^{II}$_4$(pzdz)$_4$(N$_3$)$_4$][BPh$_4$]$_4$}·4CH$_3$CN·3CHCl$_3$·2CH$_3$OH (1). Treatment of CoCl$_2$·6H$_2$O (72.5 mg, 0.31 mmol) and NaBPh$_4$ (135 mg, 0.39 mmol) in acetonitrile (5 mL) afforded a blue-greenish solution with white precipitate (NaCl), which was filtered off after 20 min.

Pzdz (90 mg, 0.31 mmol) in chloroform 5 mL, and NaN_3 (24.5 mg, 0.38 mmol) in methanol (5 mL), were added to the above solution. The resulting red solution was allowed to stand quietly for several days. Orange plate-like crystals were isolated via filtration, washed with methanol and dried in the air. Yield: 123 mg (48.3% based on Co salt). Selected IR data (cm^{-1}): 2070 (s), 1478 (m), 1432 (s), 1354 (m), 1275 (w), 1137 (w), 1094 (m), 1043 (m), 982 (m). Anal. Calcd. $C_{165}H_{166}B_4N_{40}O_2Cl_9Co_4$: C, 61.15; H, 5.20; N, 17.39. Found C, 60.71; H, 5.46; N, 17.15.

Synthesis of $\{[Co^{II}_4(pydz)_4(N_3)_4][BPh_4]_4\}\cdot 4CH_3CN$ (2). The synthesis of **2** was similar to **1** using pydz ligand instead. Orange block crystals were collected by filtration and washed with cold methanol and dried in the air. Yield 150 mg (70% based on Co salt). Selected IR data (cm^{-1}): 2065 (s), 1433 (m), 1354 (m), 986 (m). Anal. Calcd. $C_{156}H_{126}B_4Co_4N_{30}$: C, 69.40; H, 4.70; N, 15.56. Found C, 69.48; H, 4.29; N, 15.55.

Crystallography

X-ray data for **1** and **2** were collected on a Bruker D8 VENTURE diffractometer with graphite monochromated Mo Kα radiation (λ = 0.71073 Å). Lorentz/polarization corrections were applied during data reduction and the structures were solved by direct methods (SHELXS-97). Refinements were performed by full-matrix least squares (SHELXL-97)[3] on F^2 and empirical absorption corrections (SADABS)[4] were applied. Anisotropic thermal parameters were used for the non-hydrogen atoms. Hydrogen atoms were added at calculated positions and refined using a riding model. Weighted R factors (wR) and the goodness-of-fit (S) values are based on F^2; conventional R factors (R) are based on F, with F set to zero for negative F^2. CCDC-1945133 (**1**) and 1945134 (**2**) contain the crystallographic data that can be obtained via www.ccdc.cam.ac.uk/conts/retrieving.html (or from the Cambridge Crystallographic Data Centre, 12, Union Road, Cambridge CB21EZ, UK; fax: (+44) 1223-336-033; or deposit@ccdc.cam.ac.uk).

Table S1. Selected bond lengths [Å] and angles [deg] for **1**.

Co(1)-N(22)	2.175(2)	Co(2)-N(28)	2.071(2)
Co(1)-N(25)	2.076(2)	Co(2)-N(4)	2.171(2)
Co(1)-N(3)	2.157(2)	Co(2)-N(7)	2.112(2)
Co(1)-N(24)	2.119(2)	Co(2)-N(25)	2.092(2)
Co(1)-N(34)	2.078(2)	Co(2)-N(9)	2.167(2)
Co(1)-N(1)	2.122(2)	Co(2)-N(6)	2.120(2)
Co(3)-N(15)	2.171(2)	Co(4)-N(16)	2.140(2)
Co(3)-N(28)	2.064(2)	Co(4)-N(34)	2.087(2)
Co(3)-N(13)	2.146(2)	Co(4)-N(18)	2.134(2)
Co(3)-N(10)	2.161(2)	Co(4)-N(31)	2.093(2)
Co(3)-N(31)	2.095(2)	Co(4)-N(21)	2.137(2)
Co(3)-N(12)	2.112(2)	Co(4)-N(19)	2.126(2)
N(25)-Co(1)-N(22)	89.35(8)	N(28)-Co(3)-N(15)	91.21(8)
N(25)-Co(1)-N(3)	86.61(8)	N(28)-Co(3)-N(13)	93.47(8)
N(25)-Co(1)-N(24)	96.63(8)	N(28)-Co(3)-N(10)	87.13(8)
N(25)-Co(1)-N(34)	97.39(8)	N(28)-Co(3)-N(31)	97.59(8)
N(25)-Co(1)-N(1)	159.40(8)	N(28)-Co(3)-N(12)	158.46(8)

N(3)-Co(1)-N(22)	174.21(8)	N(13)-Co(3)-N(15)	73.72(8)
N(24)-Co(1)-N(22)	74.21(8)	N(13)-Co(3)-N(10)	114.38(8)
N(24)-Co(1)-N(3)	110.37(8)	N(10)-Co(3)-N(15)	171.81(8)
N(24)-Co(1)-N(1)	84.67(8)	N(31)-Co(3)-N(15)	86.13(8)
N(34)-Co(1)-N(22)	85.29(8)	N(31)-Co(3)-N(13)	157.20(8)
N(34)-Co(1)-N(3)	91.12(8)	N(31)-Co(3)-N(10)	86.13(8)
N(34)-Co(1)-N(24)	154.95(8)	N(31)-Co(3)-N(12)	91.30(8)
N(34)-Co(1)-N(1)	89.38(8)	N(12)-Co(3)-N(15)	109.02(8)
N(1)-Co(1)-N(22)	110.66(8)	N(12)-Co(3)-N(13)	85.46(8)
N(1)-Co(1)-N(3)	73.78(8)	N(12)-Co(3)-N(10)	73.88(8)
N(28)-Co(2)-N(4)	91.75(8)	N(34)-Co(4)-N(16)	86.49(8)
N(28)-Co(2)-N(7)	157.64(8)	N(34)-Co(4)-N(18)	89.80(8)
N(28)-Co(2)-N(25)	101.15(8)	N(34)-Co(4)-N(31)	102.55(8)
N(28)-Co(2)-N(9)	86.81(8)	N(34)-Co(4)-N(21)	87.17(8)
N(28)-Co(2)-N(6)	91.88(8)	N(34)-Co(4)-N(19)	159.67(8)
N(7)-Co(2)-N(4)	108.90(8)	N(18)-Co(4)-N(16)	73.96(8)
N(7)-Co(2)-N(9)	73.26(8)	N(18)-Co(4)-N(21)	108.39(8)
N(7)-Co(2)-N(6)	85.88(8)	N(31)-Co(4)-N(16)	86.91(8)
N(25)-Co(2)-N(4)	85.50(8)	N(31)-Co(4)-N(18)	156.63(8)
N(25)-Co(2)-N(7)	89.26(8)	N(31)-Co(4)-N(21)	92.16(8)
N(25)-Co(2)-N(9)	90.35(8)	N(31)-Co(4)-N(19)	85.61(8)
N(25)-Co(2)-N(6)	156.11(8)	N(21)-Co(4)-N(16)	173.24(8)
N(9)-Co(2)-N(4)	175.27(8)	N(19)-Co(4)-N(16)	112.76(8)
N(6)-Co(2)-N(4)	74.06(8)	N(19)-Co(4)-N(18)	89.48(8)
N(6)-Co(2)-N(9)	110.47(8)	N(19)-Co(4)-N(21)	73.81(8)

Table S2. Selected bond lengths [Å] and angles [deg] for **2**.

Co(1)-N(1)	2.142(1)	Co(1)-N(2)	2.124(1)
Co(1)-N(3B)	2.137(1)	Co(1)-N(4B)	2.174(1)
Co(1)-N(5)	2.068(1)	Co(1)-N(5A)	2.077(1)
N(1)-Co(1)-N(5)	92.99(5)	N(1)-Co(1)-N(5A)	157.97(5)
N(1)-Co(1)-N(2)	75.21(5)	N(1)-Co(1)-N(3B)	104.29(5)
N(1)-Co(1)-N(4B)	81.07(5)	N(2)-Co(1)-N(5)	98.58(5)
N(2)-Co(1)-N(4B)	101.10(5)	N(2)-Co(1)-N(5A)	85.84(5)
N(2)-Co(1)-N(3B)	175.65(5)	N(3B)-Co(1)-N(5A)	93.75(5)
N(3B)-Co(1)-N(4B)	74.57(5)	N(3B)-Co(1)-N(5)	85.76(5)
N(4B)-Co(1)-N(5)	157.19(5)	N(4B)-Co(1)-N(5A)	91.90(5)
N(5)-Co(1)-N(5A)	100.96(7)		

Symmetry transformations used to generate equivalent atoms:

A: y+1/4, -x+7/4, -z+3/4   B: -y+7/4, x-1/4, -z+3/4

**Table S3**. Parameters fitted by a generalized Debye model for **1** at 1500 Oe dc field.

T / K	τ / s	α
2.0	1.02×10^{-1}	0.39
2.1	6.29×10^{-2}	0.39
2.2	3.52×10^{-2}	0.39
2.3	1.85×10^{-2}	0.38
2.4	1.04×10^{-2}	0.37
2.5	5.65×10^{-3}	0.36
2.6	3.23×10^{-3}	0.35
2.7	1.88×10^{-3}	0.35
2.8	1.17×10^{-3}	0.34
2.9	7.43×10^{-4}	0.33
3.0	4.96×10^{-4}	0.31
3.1	3.29×10^{-4}	0.31
3.2	2.27×10^{-4}	0.30
3.3	1.59×10^{-4}	0.28
3.4	1.25×10^{-4}	0.26

Table S4. Parameters fitted by a generalized Debye model for **2** at 2000 Oe dc field.

T / K	τ / s	α
3.0	7.73×10^{-2}	0.32
3.1	3.99×10^{-2}	0.26
3.2	2.29×10^{-2}	0.21
3.3	1.40×10^{-2}	0.16
3.4	8.70×10^{-3}	0.14
3.5	5.62×10^{-3}	0.12
3.6	3.64×10^{-3}	0.10
3.7	2.42×10^{-3}	0.09
3.8	1.63×10^{-3}	0.08
3.9	1.11×10^{-3}	0.06
4.0	7.74×10^{-4}	0.05
4.1	5.50×10^{-4}	0.04
4.2	3.96×10^{-4}	0.03
4.3	2.78×10^{-4}	0.05
4.4	1.97×10^{-4}	0.06
4.5	1.33×10^{-4}	0.07
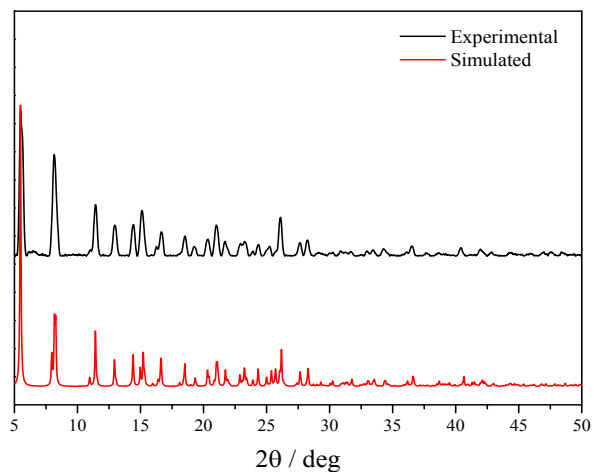
Fig. S1 Powder X-ray diffraction pattern and the simulation from the single crystal data of **2**.
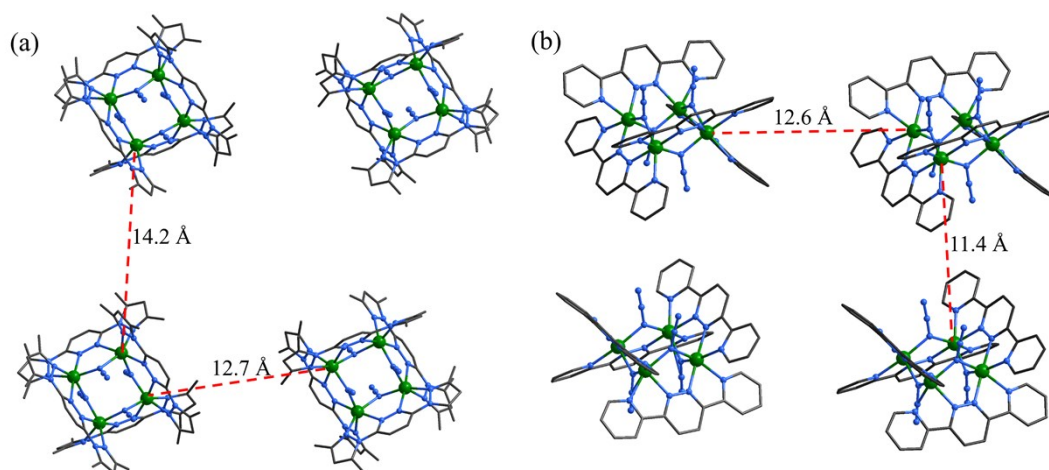

Fig. S2 The packing diagram of **1** (a) and **2** (b). The dashed line shows the nearest intermolecular Co···Co separation. Hydrogen atoms, counter anions and interstitial solvent molecules are omitted for clarify. Colour codes: Co(II), green; C, grey; N, light blue.
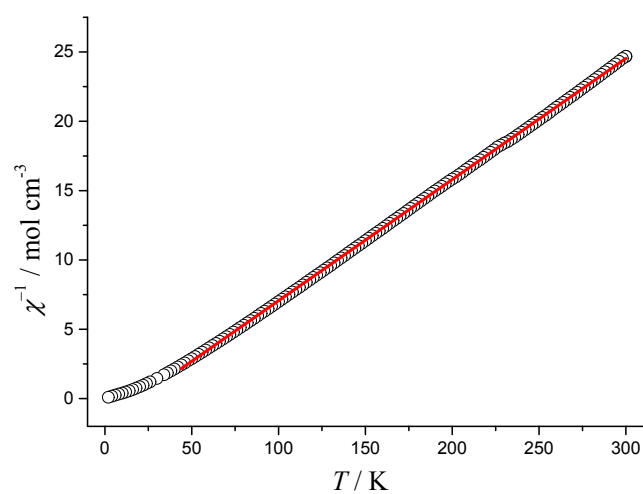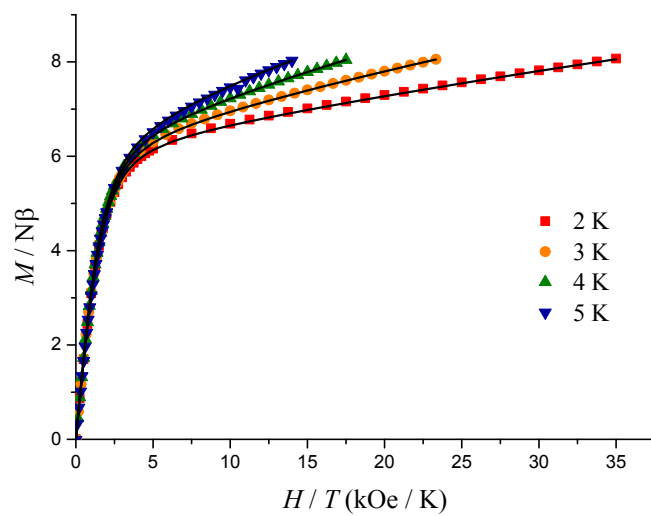

Fig. S3 Temperature dependent χ^{-1} plots for **1** measured at 1000 Oe dc field. The red line represents the Curie-Weiss fit to the data.
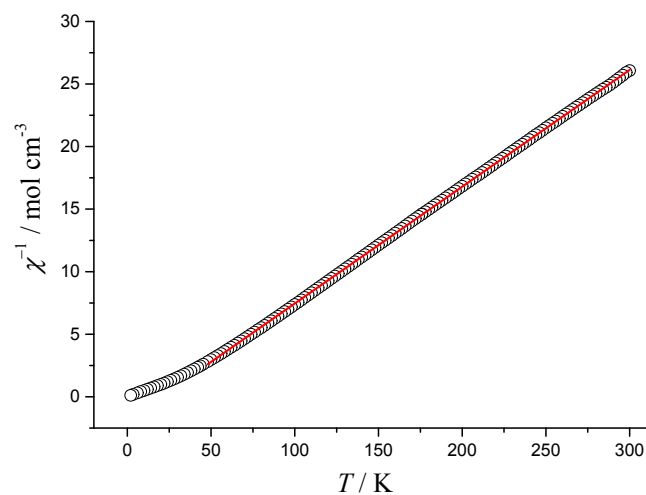
Fig. S4 Temperature dependent χ^{-1} plots for **2** measured at 1000 Oe dc field. The red line represents the Curie-Weiss fit to the data.
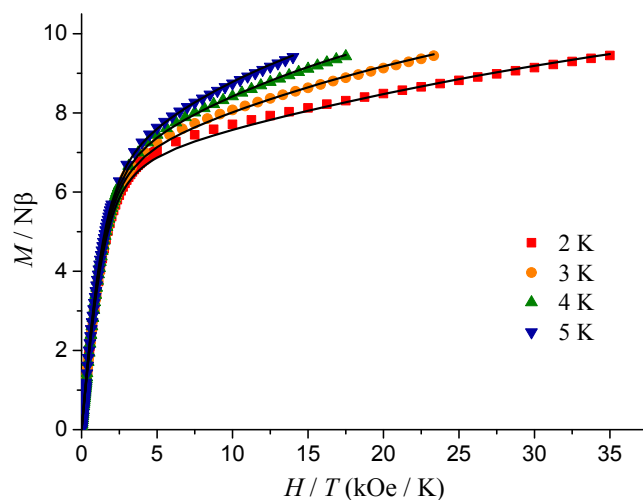
Fig. S5 Reduced magnetization data for **1** at 2-5 K. The solid lines represent the fit to the data.

Fig. S6 Reduced magnetization data for **2** at 2-5 K. The solid lines represent the fit to the data.
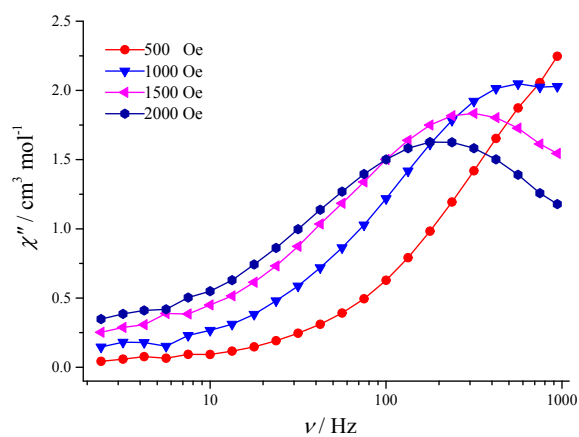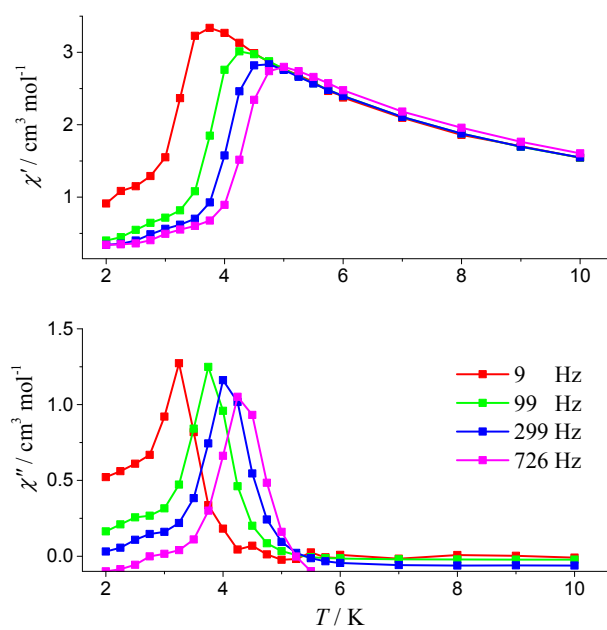
Fig. S7 Frequency dependence of the out-of-phase (χ'') ac susceptibility for **1** as a function of applied field at 3 K. The lines are guides to the eye.
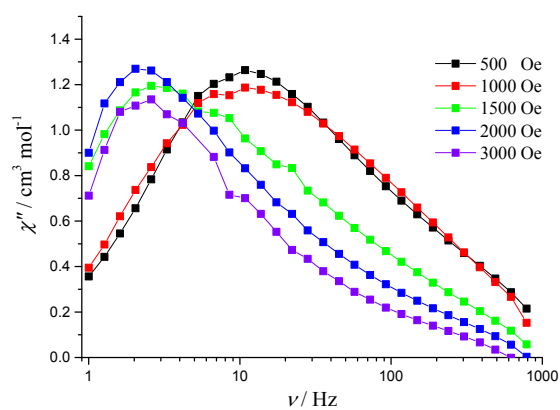
Fig. S8 Frequency dependence of the out-of-phase (χ'') ac susceptibility for **2** as a function of applied field at 3 K. The lines are guides to the eye.
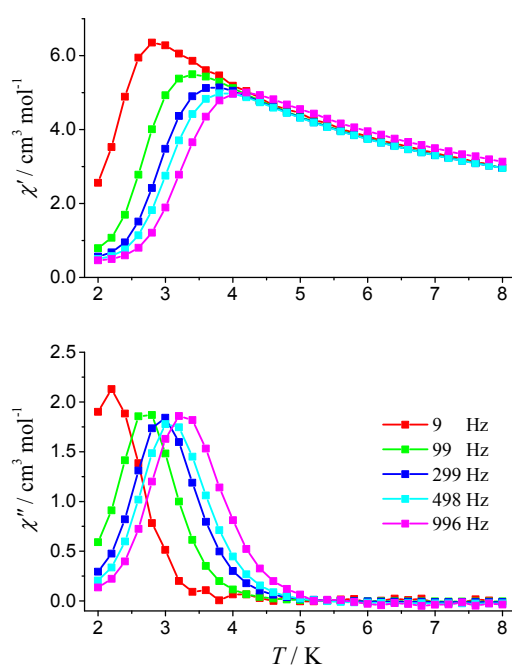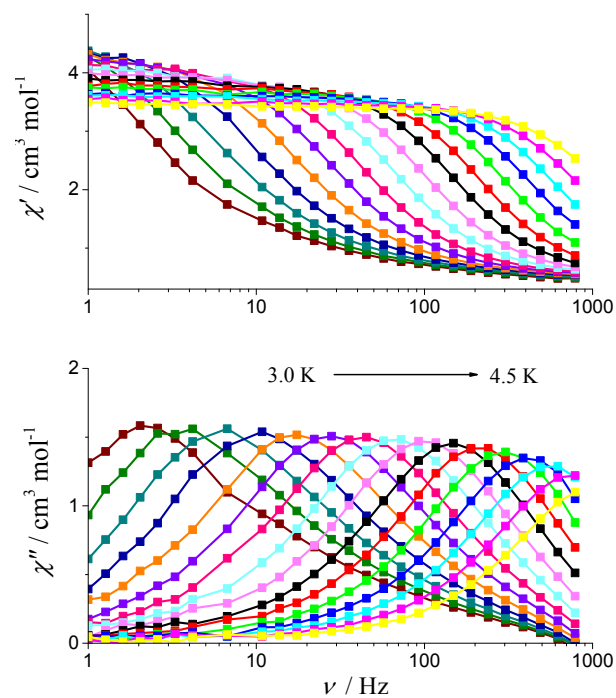

Fig. S9 Temperature dependence of the in-phase (χ') and out-of-phase (χ'') ac susceptibility for **1** under 1500 Oe dc field. Solid lines are guides for the eye.

Fig. S10 Temperature dependence of the in-phase (χ') and out-of-phase (χ'') ac susceptibility for **2** under 2000 Oe dc field. Solid lines are guides for the eye.
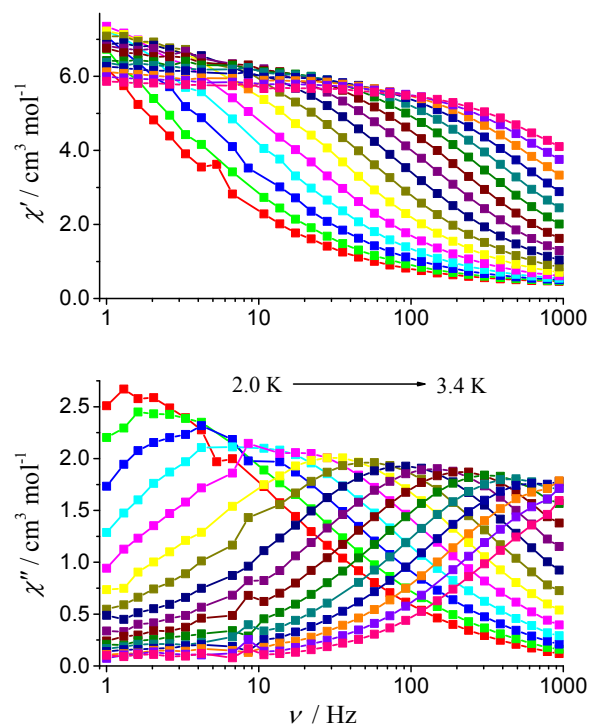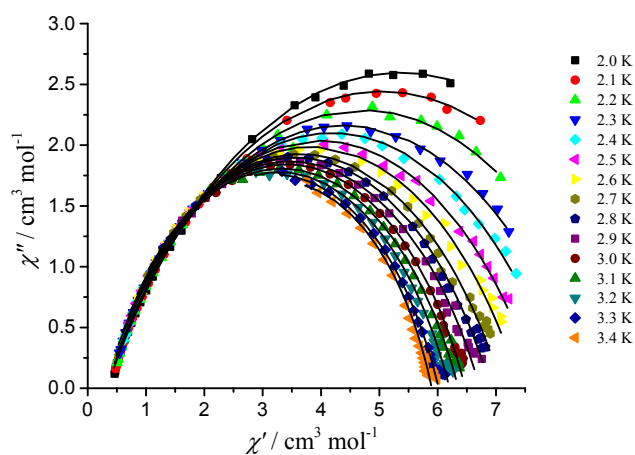

Fig. S11 Frequency dependence of the in-phase (χ') and out-of-phase (χ'') ac susceptibility for **1** under 1500 Oe dc field. Solid lines are guides for the eye.
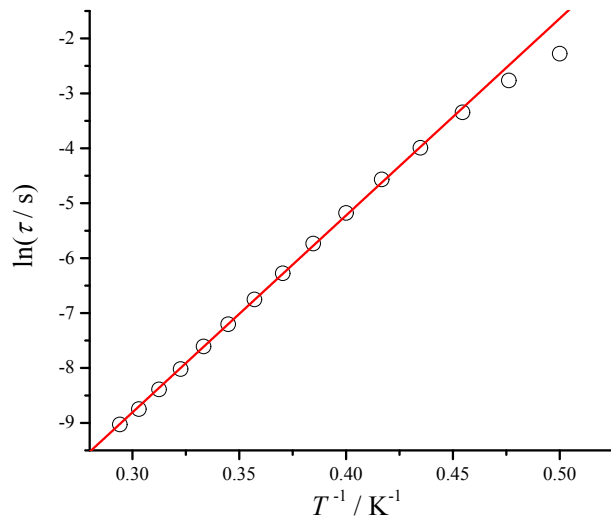
Fig. S12 Frequency dependence of the in-phase (χ') and out-of-phase (χ'') ac susceptibility for **2** under 2000 Oe dc field. Solid lines are guides for the eye.
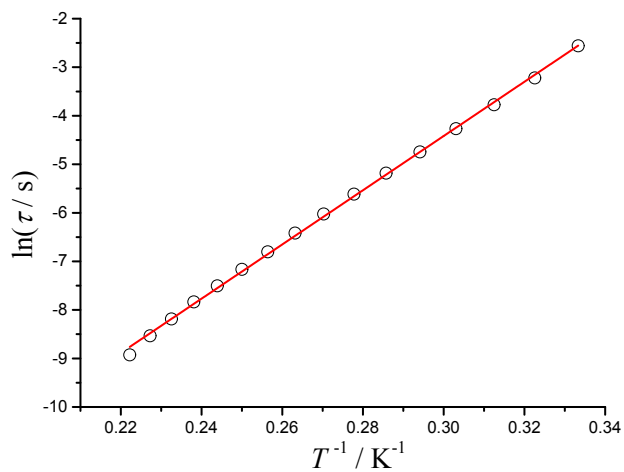

Fig. S13 Cole-Cole plots of **1** under 1500 Oe dc field. The lines represent the fit to the data.
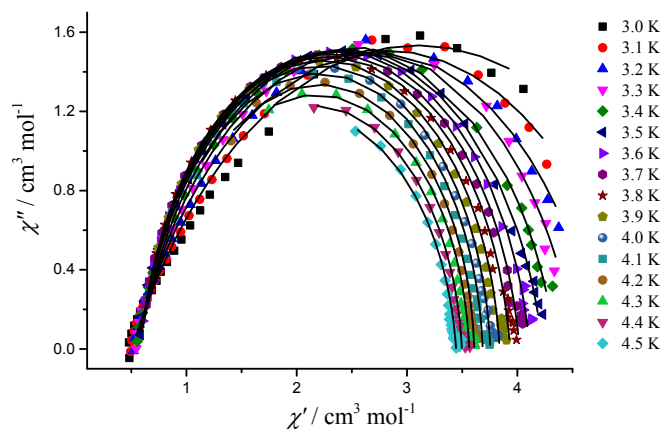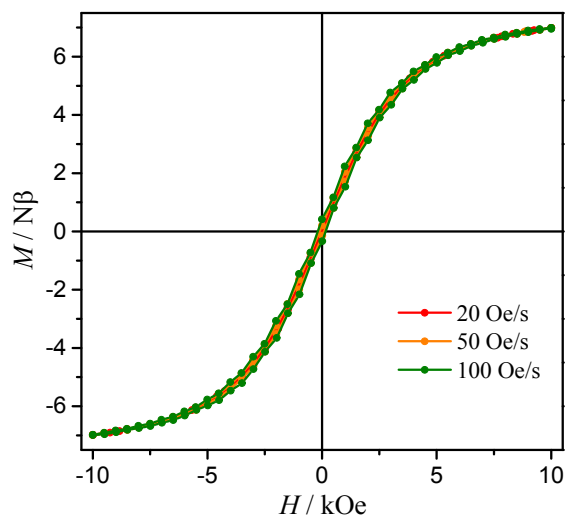

Fig. S14 Cole-Cole plots of **2** under 2000 Oe dc field. The lines represent the fit to the data.
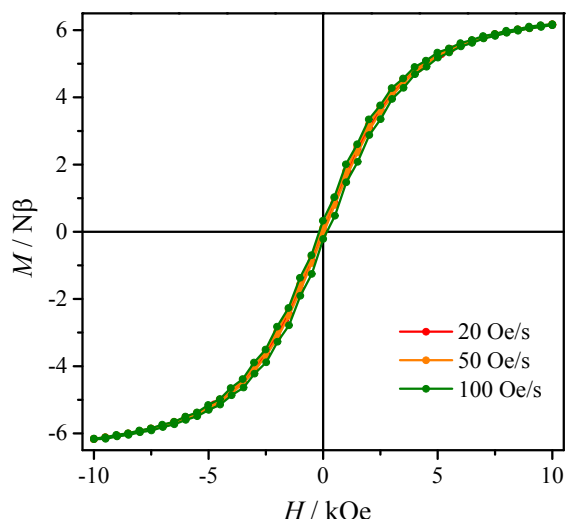
Fig. S15 Temperature dependence of the relaxation time for **1** under 1500 Oe dc field. The line represents the fit by Arrhenius Law.

Fig. S16 Temperature dependence of the relaxation time for **2** under 2000 Oe dc field. The line represents the fit by Arrhenius Law.

Fig. S17 Magnetic hysteresis measurements of **1** recorded at 2.0 K with field sweep rate of 20, 50 and 100 Oe/s.

Fig. S18 Magnetic hysteresis measurements of **2** recorded at 2.0 K with field sweep rate of 20, 50 and 100 Oe/s.

References

1   L. K. Thompson, T. C. Woon, D. B. Murphy, E. J. Gabe, F. L. Lee, and Y. Le Page, *Inorg. Chem.* 1985, **24**, 4719.

2   G. A. Bain and J. F. Berry, *J. Chem. Educ.*, 2008, **85**, 532.

3   (a) Sheldrick, G. M., SHELXL-2014, Program for the solution of crystal structures. University of Göttingen, Göttingen, Germany, 2014; (b) Sheldrick, G. M., SHELXL-2014, Program for Crystal Structure Refinement. University of Göttingen, Göttingen, Germany, 2014.

4   Sheldrick, G. M., SADABS, v.2.01, Bruker/Siemens Area Detector Absorption Correction Program. Bruker AXS: Madison, Wisconism, 1998.